NOLTR 72-103

THE UNDERPRESSURE FIELD FROM EXPLOSIONS IN WATER AS MODIFIED BY CAVITATION

By
J. B. Gaspin
R. S. Price

9 MAY 1972

NOL

NAVAL ORDNANCE LABORATORY, WHITE OAK, SILVER SPRING, MARYLAND

NOLTR 72-103

UNCLASSIFIED

Security Classification

DOCUMENT CONTROL DATA - R & D

(Security classification of title, body of abstract and indexing annotation must be entered when the overall report is classified)

1 ORIGINATING ACTIVITY (Corporate author)	2a. REPORT SECURITY CLASSIFICATION
Naval Ordnance Laboratory White Oak, Silver Spring; Md 20910	UNCLASSIFIED
	2b. GROUP

3 REPORT TITLE

The Underpressure Field from Explosions in Water as Modified by Cavitation

4 DESCRIPTIVE NOTES *(Type of report and inclusive dates)*

5 AUTHOR(S) *(First name, middle initial, last name)*

J. B. Gaspin and R. S. Price

6 REPORT DATE	7a. TOTAL NO. OF PAGES	7b. NO. OF REFS
9 May 1972	iii + 23	8

8a CONTRACT OR GRANT NO	9a. ORIGINATOR'S REPORT NUMBER(S)
b. PROJECT NO. ORD-0332-004/092-1/UF 554-201	NOLTR 72-103
c.	9b OTHER REPORT NO(S) *(Any other numbers that may be assigned this report)*
d.	

10 DISTRIBUTION STATEMENT

Approved for public release; distribution unlimited

11 SUPPLEMENTARY NOTES	12 SPONSORING MILITARY ACTIVITY
	Naval Ordnance Systems Command Washington, D.C.

13 ABSTRACT

Existing bulk cavitation theory has been used to map the extent of the cavitated region caused by an underwater explosion and to calculate the underpressure level of the surface reflected shock wave as modified by cavitation. The calculation of the cavitation boundaries has not been verified experimentally. The calculated values of the underpressures compare well with experimental values.

Ia

DD FORM 1 NOV 65 1473 (PAGE 1)

S/N 0101-807-6801

UNCLASSIFIED

Security Classification

14 KEY WORDS	LINK A		LINK B		LINK C	
	ROLE	WT	ROLE	WT	ROLE	WT
Underwater Explosions						
Bulk Cavitation						
Underpressure Calculations						
Surface						
Reflection						
Shock Waves						

Ih

THE UNDERPRESSURE FIELD FROM EXPLOSIONS IN WATER AS MODIFIED BY CAVITATION

by
J. B. Gaspin and R. S. Price

ABSTRACT Existing bulk cavitation theory has been used to map the extent of the cavitated region caused by an underwater explosion and to calculate the underpressure level of the surface reflected shock wave as modified by cavitation. The calculation of the cavitation boundaries has not been verified experimentally. The calculated values of the underpressures compare well with experimental values.

NAVAL ORDNANCE LABORATORY
White Oak, Silver Spring, Maryland
EXPLOSIONS RESEARCH DEPARTMENT
UNDERWATER EXPLOSIONS DIVISION

NOLTR 72-103 **9 May 1972**

The Underpressure Field from Explosions in Water as Modified by Cavitation

This work was done as part of a study of the effects of underwater explosion pressure waves on marine organisms. It was funded by the Naval Ordnance Systems Command under Task Assignment ORD-0332-004/092-1/UF 554-201 (Environmental Effect of Explosive Testing).

Subsequently, this work has been useful in achieving a better understanding in the "anomalies" of the pressure wave shapes obtained on another project. It is being presented as an NOL Technical Report with the expectation that it may be helpful to others who are working in related fields.

The authors are grateful to Miss E. A. Christian for many helpful discussions and suggestions.

ROBERT WILLIAMSON II
Captain, USN
Commander

C. J. Aronson

C. J. ARONSON
By direction

CONTENTS

ILLUSTRATIONS

TABLES

THE UNDERPRESSURE FIELD FROM EXPLOSIONS IN WATER AS MODIFIED BY CAVITATION

1. INTRODUCTION

In connection with a current study of the effects of underwater explosion pressure waves on marine organisms, it was desired to determine the effect of bulk cavitation on the pressure field. In particular, since the negative-going, surface-reflected shock wave has been suggested as an important element in damage production to some classes of fish, the prediction of these negative pressures was undertaken. Existing cavitation theory has been used to map the cavitated region for several geometries of interest. Negative pressure amplitudes beneath the cavitated region have been calculated using two different approachs in addition to that suggested by Arons, et al, (Ref 1); the results of the three approaches are compared with some existing data.

2. CAVITATION THEORY

If cavitation is not considered, the amplitude of the surface reflected shock wave is usually calculated by assuming a negative-going image source of strength equal to the actual source. Since the occurence of cavitation markedly reduces the strength of the reflected wave, non-cavitation predictions are unrealistic.

The history of cavitation theory shows no lack of effort, especially since World War II. References 1 through 8 are only a few of the papers existing which cover aspects of cavitation theories. In actuality, the groundwork for all these theories was laid by Kennard in two papers in 1943 [2,3]. While there have been refinements and additions to this work (especially as concerns the dynamics of the cavitated region after initial formation, which is of little interest for the application of this report), the basic assumptions bearing on the formation of the cavitated region have remained unchanged (as well as untested by experiment). The development presented below follows that of Arons, et al [1]. This treatment was chosen for its conceptual and computational simplicity.

Reference 1 makes three basic assumptions:

(a) "Cavitation begins when the pressure in the water drops to a fixed value, Pc, the cavitation pressure. We will take Pc = 0 psi."

(b) "The pressure at a point on the front of the reflected wave can be described as emanating from an image charge above the surface, having a variable apparent weight, Wi, so adjusted as to account for the pressure diminution due to cavitation."

(c) "Wi is a continuous non-increasing function of distance along a ray away from the image charge, being equal to the true charge weight, W, before any cavitation takes place, decreasing monotonically in regions of cavitation, and remaining constant in regions of no cavitation."

The total pressure in the water, before cavitation has occurred, is given by the sum of the direct, surface-reflected, and hydrostatic pressures. Assuming for calculational convenience that the shock wave is an instantaneous rise to a peak pressure, followed by an exponential decay of time constant θ, the pressure at a point in the water at the time of arrival of the surface reflection is:

$$P_o e^{-t/\theta} + P_r + P_z, \tag{1}$$

where P_o is the shock wave peak pressure, t is the time delay between the direct and surface-reflected arrivals, P_r is the surface-reflected peak pressure, and P_z is the hydrostatic pressure. Actually the relationship for pressure as a function of time in the shock wave is only good until the time is about one θ; at later times the pressure may be well above the calculated value. For calculating pressures in the immediate vicinity of the cavitation region it is probably quite adequate. According to assumption (a) we have:

$$P_o e^{-t/\theta} + P_r + P_z = 0 \tag{2}$$

The coordinate system to be used in the following calculation is shown in Figure 1.

Assuming that the shock wave peak pressure may be calculated from a similitude equation of the form:

$$P = K \left(\frac{W^{1/3}}{R}\right)^{1.13}, \tag{3}$$

we have

$$P_o = K \left(\frac{W^{1/3}}{R_1}\right)^{1.13} \quad \text{and} \tag{4}$$

$$P_r = K \left(\frac{Wi^{1/3}}{R_2}\right)^{1.13}, \tag{5}$$

where K is an empirical constant depending on the explosive composition, R, is the slant range from charge to gage, and R_2 is the slant range from image to gage. In addition, the hydrostatic pressure, P_z, may be assumed given by:

$$P_z = P_a + H (R_1 \cos \alpha - d), \tag{6}$$

where P_a is the atmospheric pressure, d is the charge depth, H is a constant, and α is the angle between the line from image to gage and a vertical line through image and charge.

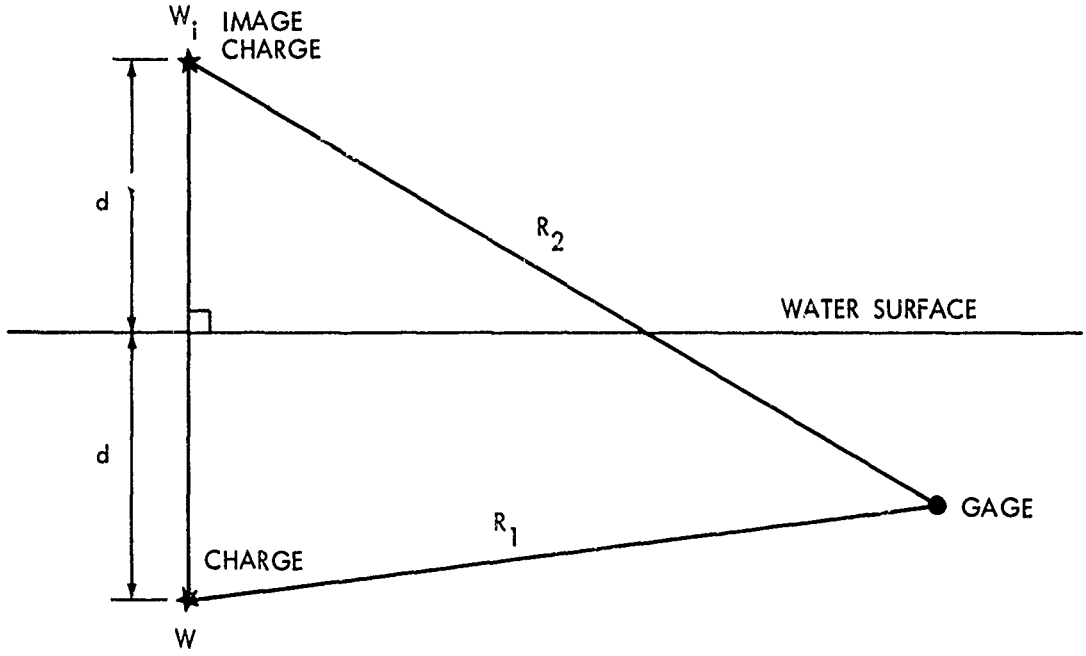

FIG. 1 COORDINATE SYSTEM FOR CAVITATION CALCULATION

Combining equations 2, 4, 5, and 6, we have:

$$K\left(\frac{W^{1/3}}{R_1}\right)^{1.13} e^{-t/\theta} - K\left(\frac{Wi^{1/3}}{R_2}\right)^{1.13} + P_a + H\,(R_2 \cos\alpha - d) = 0 \qquad (7)$$

Solving for the variable image weight,

$$W_i = \left\{\frac{R_2^{1.13}}{K}\left[P_a + H\,(R_2 \cos\alpha - d) + K\left(\frac{W^{1/3}}{R}\right)^{1.13} e^{-t/\theta}\right]\right\}^{\frac{3.00}{1.13}} \qquad (8)$$

The arrival difference, t, is given by:

$$t = \frac{R_1 - R_2}{C}, \qquad (9)$$

where C is the velocity of sound in water. The cavitation region may now be mapped using assumptions (b) and (c). At a fixed α, allowing R_2 to vary, the upper surface of the cavitated region is found by setting:

$$W_i = W \qquad (10)$$

The bottom of the cavitated region is found when

$$\frac{dW_i}{dR_i} = 0 \qquad (11)$$

Following rays from the image charge of different angles α, the entire cavitation zone may be mapped out. To calculate the negative underpressure at points below the cavitated region using the approach suggested by Arons, et al, the image weight corresponding to equation 11 is used, and spherical spreading is utilized to extrapolate from the underpressure at the bottom of the cavitated zone to the desired point in the water.

One modified approach, Gaspin-Price plane wave, assumes that the amplitude of the negative wave is determined at the bottom of the cavitation zone in the manner outlined above. The wave then continues to propagate radially from the image source but as a plane wave with its origin the bottom surface of the cavitated region. It is obvious that this is not completely realistic, but it seems to be closer to reality than assuming a point source with spherical spreading. Specifically, it should be better at positions beneath the central portion of the cavitated region (such as f in Figure 2(a)). The assumption of plane wave propagation probably becomes less valid when the radial line from the image source passes through the extremities of the cavitation region (as at g in Figure 2(a)).

The duration of the negative phase is determined by the time that the cavitation remains open, i.e., until cavitation closure occurs along the ray connecting the image to the gage.

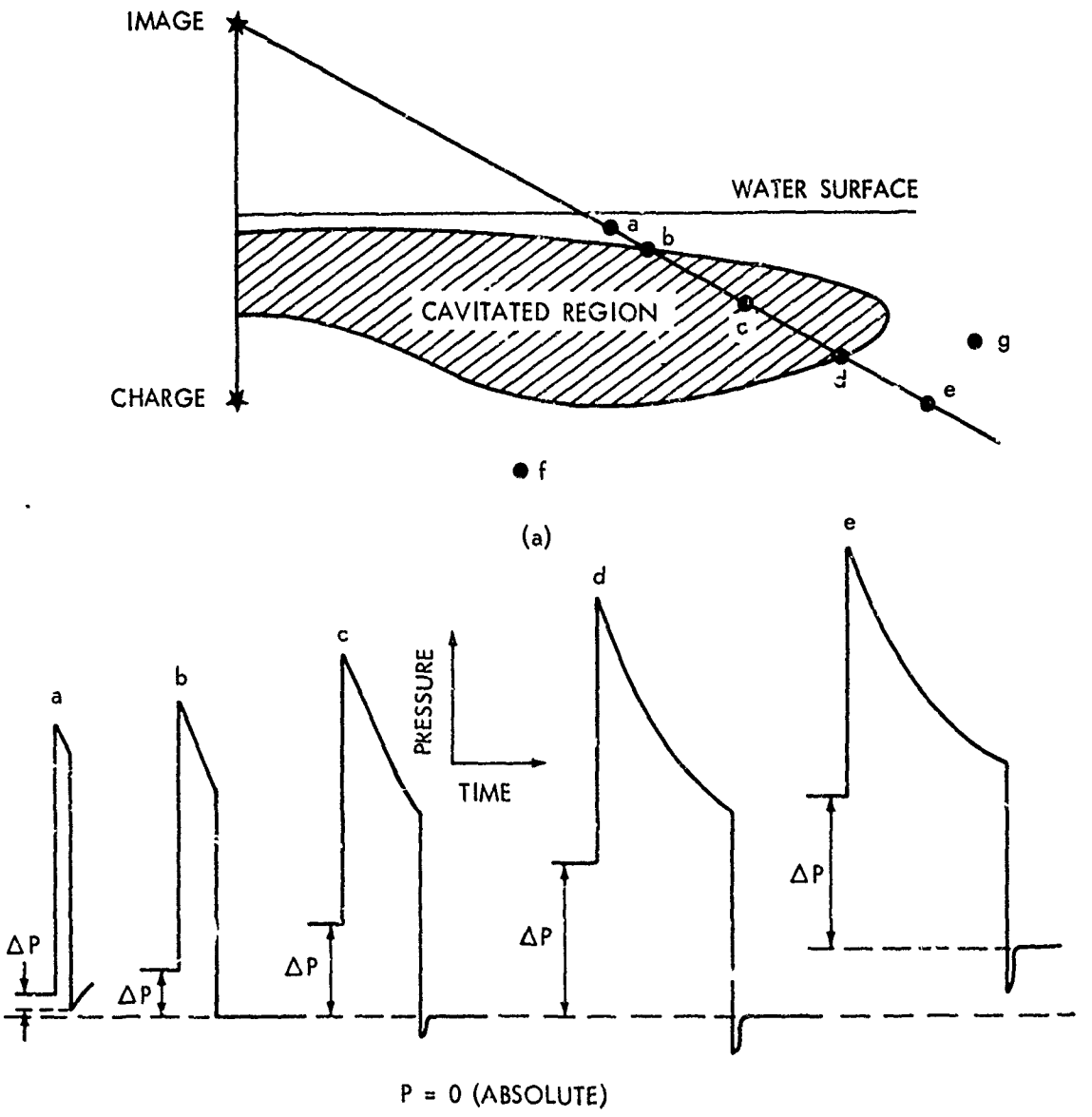

FIG. 2 WAVEFORMS AS MODIFIED BY CAVITATION

There are undoubtedly limits to the regions below, and just out-from-under, the cavitation zone in which the modified approach may be used. The limitations have to be set by appropriate analytical and experimental methods.

Another approach, the hydrostatic origin approximation, assumes that the calculated negative pressure at the bottom of the cavitation region directly above the point of interest (a gage for example) is propagated downward as a plane wave. Essentially the pressure due to water and atmosphere above the cavitation region is removed from the water column below the cavitation. The pressure is removed until the loading pressures and cavitation closure restore conditions to a more nearly normal state. The long duration and even pressure in the early parts of the negative phase are thus explained.

This approximation must break down at great depths and at positions horizontally beyond the cavitated region.

3. MODIFICATION OF THE SURFACE REFLECTED WAVE FORM BY CAVITATION

Figure 2 illustrates the manner in which the wave form of the surface reflected shock wave is modified by cavitation. The five pressure-time curves are lettered to correspond to the five successively deeper points indicated in the sketch. At point "a", the surface reflection does not lower the pressure as far as absolute zero, and no cavitation occurs. At this point, the surface reflected pressures may be reasonably calculated assuming an image source of equal strength to the actual source, and a negative exponential wave form. At point "b", on the upper edge of the cavitated zone, the reflected pressure is just sufficient to lower the total pressure to absolute zero and cavitation occurs. After the pressure reaches zero, it stays relatively stable at that level and eventually merges into succeeding events (closure). At points "c" and "d", within and on the lower boundary of the region, the reflected wave form shows a sharp negative spike below absolute zero. This net tension results from the finite time necessary for the water to cavitate. On many recordings, this spike is not apparent due to inadequate frequency response. Following this spike, the pressure returns to a more or less stable "plateau" pressure of absolute zero. As the wave propagates to point "e", the wave form retains the general features which characterized "c" and "d", but the reflected pressure is no longer adequate to produce cavitation.

The underpressure at points b, c, and d may easily be calculated. The total pressure at these points reaches absolute zero, so the underpressure, is just equal to the hydrostatic pressure at these depths. At point "e", the pressure may be calculated either using the image weight obtaining at point "d", and allowing for diminution of the underpressure due to spherical spreading between points "d" and "e", or by calculating the underpressure at "d" and assuming that this underpressure propagates as in plane wave to "e." We have not found data to check conditions at a point such as "e" which is not under the cavitated region.

4. RESULTS

Computer programs have been written to calculate the negative pressure below the cavitated region and the boundary of the region; they are listed in the appendices. They are written in BASIC and have been run on the CDC 6400 computer.

The cavitated region has been mapped for several conditions of interest, as shown in Figures 3 through 6. As mentioned above, this calculation is essentially unchecked by experiment. The experiment described in reference 6 roughly confirmed the calculation of the upper boundary of the cavitated region, but to the authors knowledge, the calculation of the lower boundary has never been experimentally verified. No data is presently available to make a direct verification.

Data is available, however, to compare with calculations of the magnitude of the underpressure below the cavitated region. Computer programs were written to make this calculation, and several samples of available data were analyzed to determine the negative "plateau" underpressure. These measurements are of a rather crude nature, since the instrumentation was set up to record the much higher amplitude of the direct shock wave, and the negative pressures are a small fraction of the full scale reading. They do, however, give some indication that the calculations of underpressures are valid, particularly if plane wave propagation is assumed, and thus provide an indirect verification of the calculation of the lower cavitation boundary. Table I and Figures 7 through 10 present this comparison. Also indicated in Table I are the corresponding underpressure as calculated by assuming an image source of strength equal to the actual charge (no provision being made for cavitation). It is clear that the cavitation calculations give a much more accurate representation of the measured pressures. Since data from charges of 0.49 and 4×10^4 pounds are reasonably well predicted, the present calculation is considered adequate for purposes of experimental design. A more extensive comparison would be desirable, however. The fact that these pressures are reasonably well modeled, and that the position of the lower boundary influences these pressures, indicates, albeit indirectly, that there probably is some validity to the lower boundary calculation.

5. CONCLUSION

Existing bulk cavitation theory may be used to predict the extent of the cavitated region caused by underwater explosions and also the negative pressure amplitudes below the cavitated region. While the calculation of the extent of the region is largely untested by experiment, preliminary comparisons with data indicate that these calculations of the underpressure amplitudes are a considerable improvement over calculations made without considering cavitation.

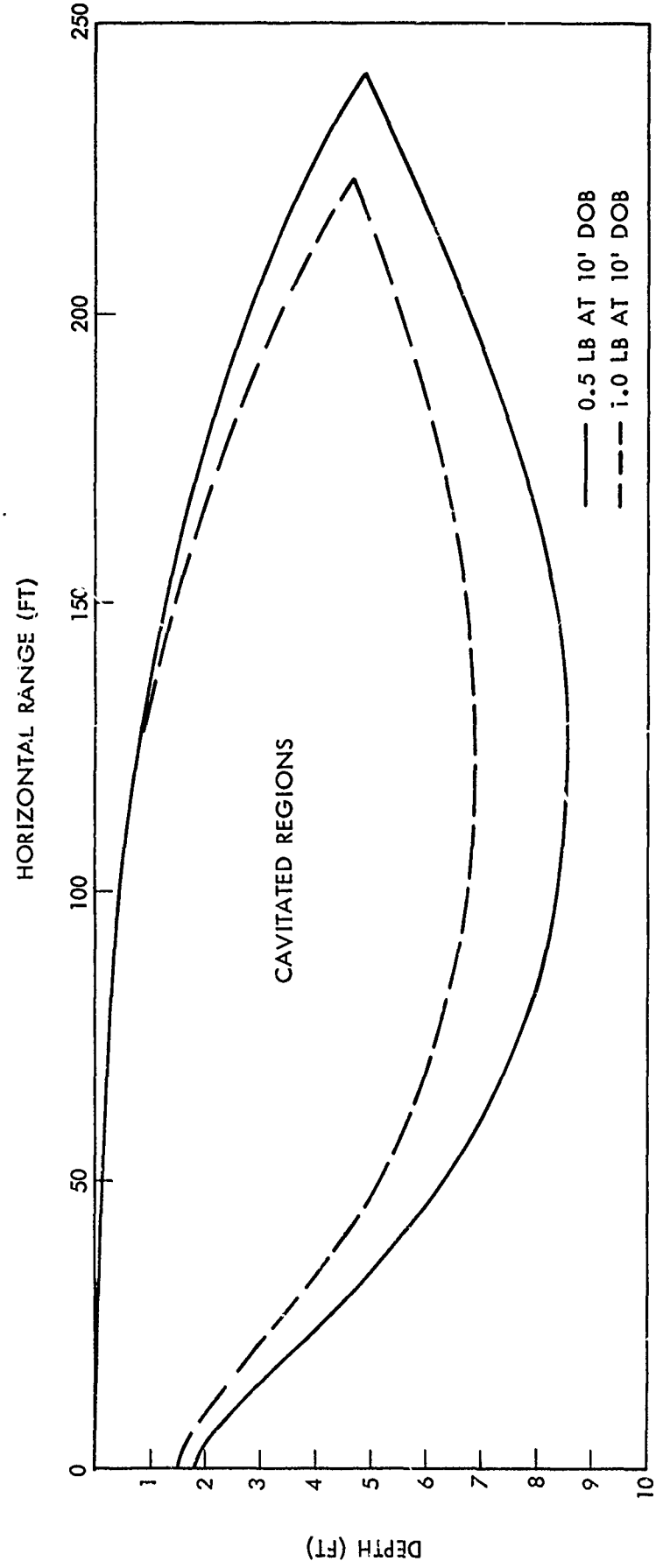

FIG. 3 BOUNDARY OF CAVITATED REGION

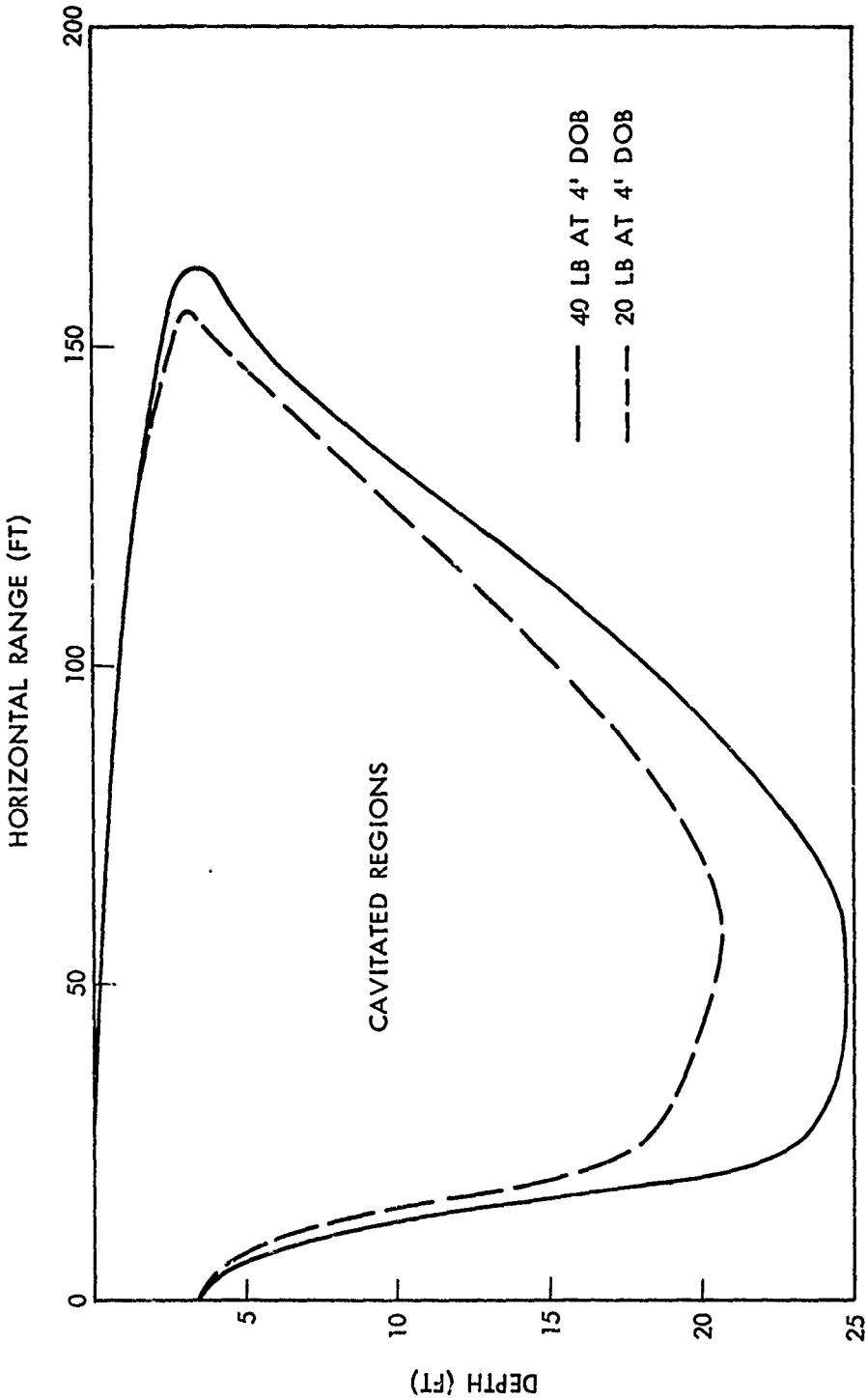

FIG. 4 BOUNDARY OF CAVITATED REGION

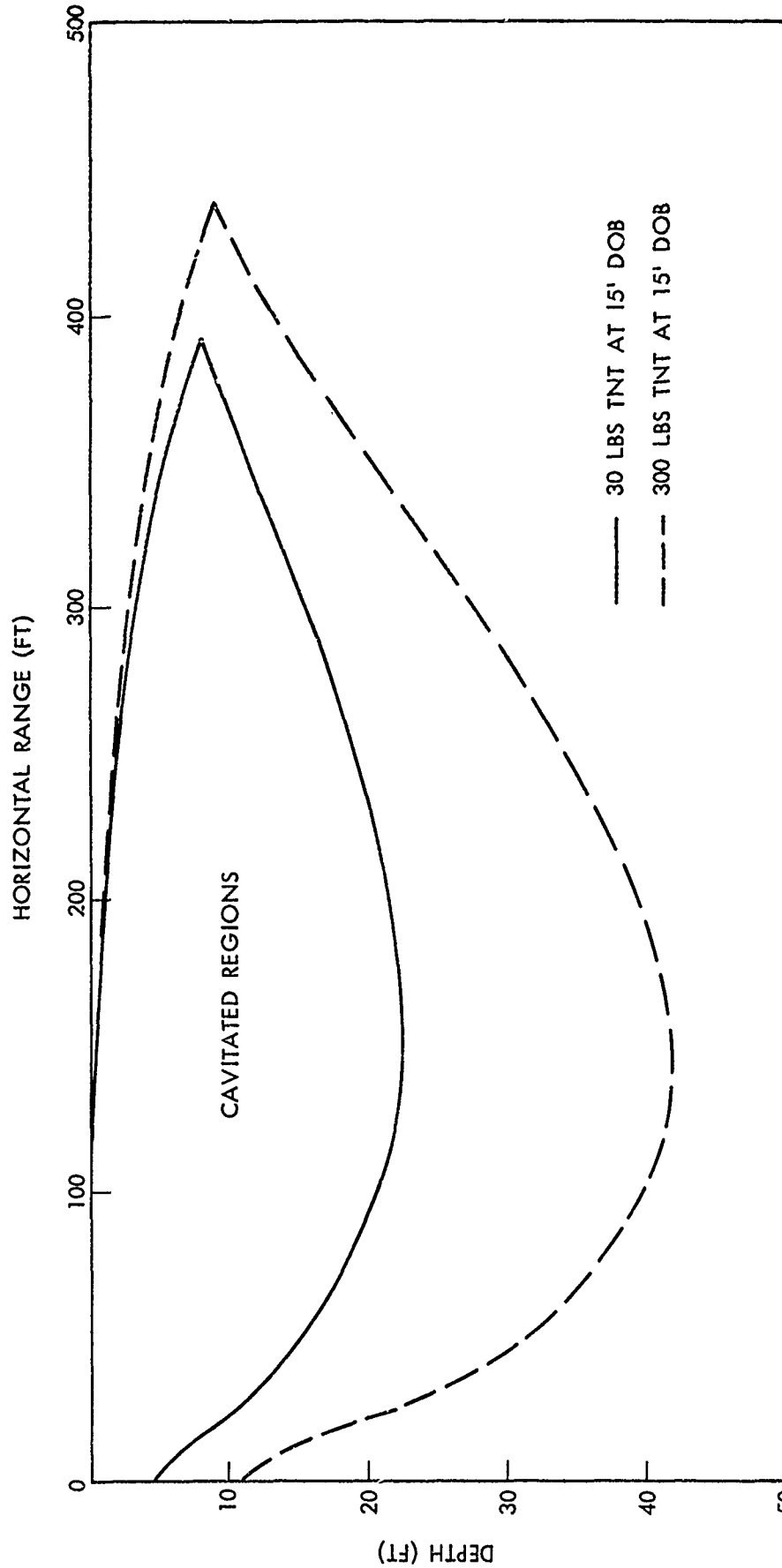

FIG. 5 BOUNDARY OF CAVITATED REGION

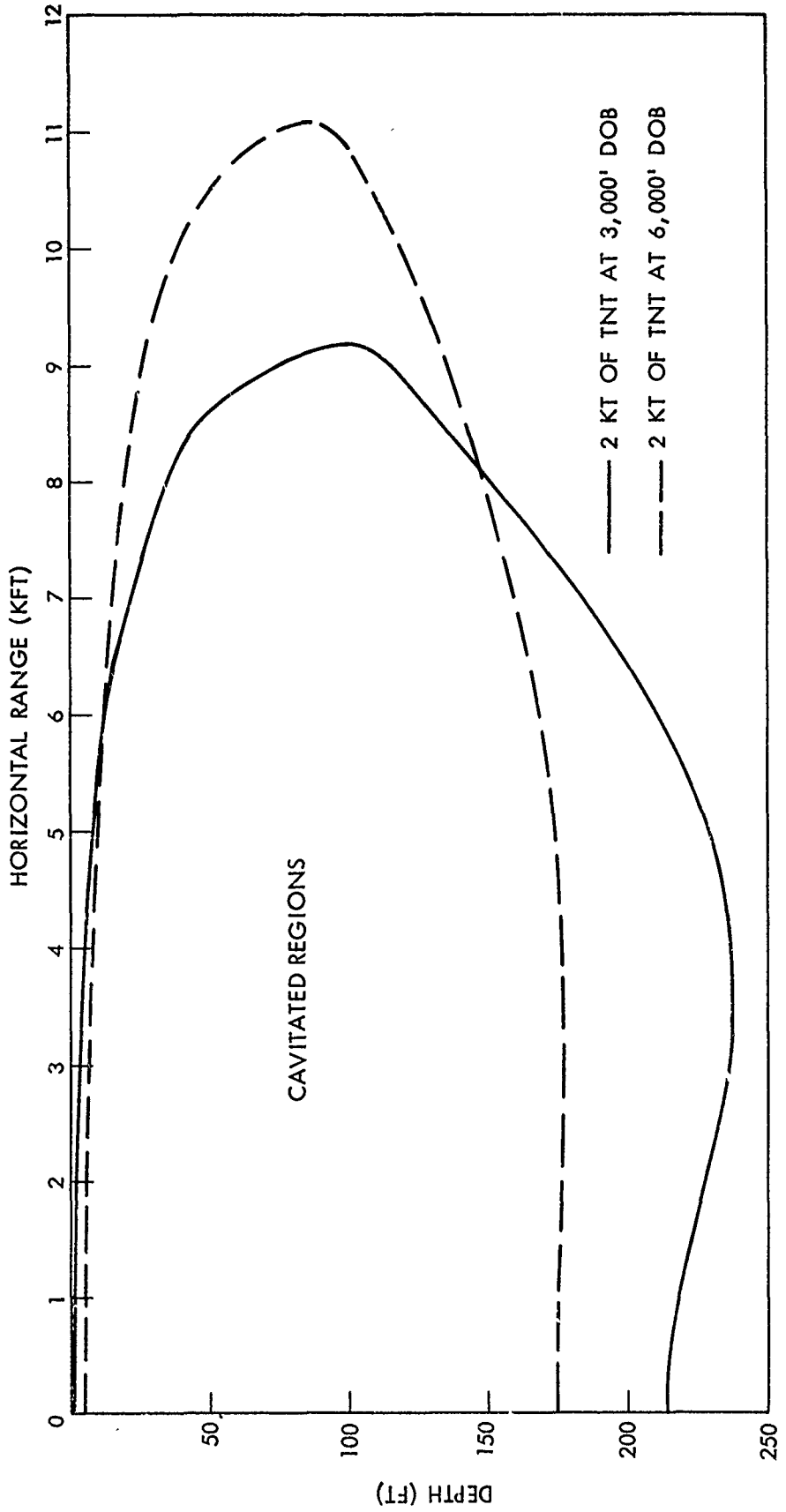

FIG. 6 BOUNDARY OF CAVITATED REGION

TABLE I. UNDERPRESSURE COMPARISONS

Pressures in psi

Charge Weight (lbs)	Charge Depth (ft)	Horizontal Range (ft)	Gage Depth (ft)	Negative Pressures Calculated (a)	(b)	(c)	(d)	measured
40,000	200	1019	220	-71	-78	-80	-436	-88
			281	-71	-69	-77	-436	-84
			342	-71	-58	-76	-429	-72
			403	-71	-50	-74	-419	-75
			464	-71	-42	-73	-408	-71
			525	-71	-36	-71	-396	-76
			585	-71	-32	-70	-384	-81
			647	-71	-28	-69	-372	-76
			678	-71	-26	-68	-366	-80
			708	-71	-25	-66	-360	-53
40,000	200	570	220	-66	-60	-71	-735	-81
			281	-66	-48	-68	-676	-78
			342	-66	-40	-66	-657	-69
			403	-66	-33	-65	-620	-62
			464	-66	-29	-63	-585	—
			525	-66	-25	-61	-552	-81
			585	-66	-22	-60	-522	-70
			647	-66	—	—	—	*
			678	-66	-19	-59	-481	*
			708	-66	-18	-58	-469	*
40,000	200	407	220	-61	-48	-65	-907	-80
			281	-61	-39	-63	-837	-71
			342	-61	-33	-61	-773	-96
			403	-61	-28	-59	-716	—
			464	-61	—	—	—	—
			525	-61	-22	-57	-618	-70
			585	-61	-20	-56	-578	*
			647	-61	-18	-55	-542	*
			673	-61	-17	-55	-524	*
			708	-61	-16	-54	-509	*

TABLE I. UNDERPRESSURE COMPARISONS (continued)

Pressures in psi

Charge Weight (lts)	Charge Depth (ft)	Horizontal Range (ft)	Gage Depth (ft)	Negative Pressures Calculated (a)	(b)	(c)	(d)	measured
10,000	200	534	220	-48	-33	-52	-466	-50
			281	-48	-27	-49	-438	-48
			342	-48	-23	-47	-412	-45
			403	-48	-19	-46	-387	-57
			464	-48	-17	-45	-364	-44
			525	-48	-15	-43	-342	-41
			585	-48	-14	-43	-324	-36
			647	-48	-12	-42	-305	*
			678	-48	-12	-42	-297	*
			708	-48	-11	-41	-289	*
.06	10	48	10	-16	-15	-16	-244	-19
1.05	10	84	10	-19	-18	-19	-133	-21
0.49	10	100	10	-18	-17	-18	-83	-17

(a) Hydrostatic Origin Approximation

(b) Arons-Gaspin Spherical Spreading

(c) Gaspin-Price Plane Wave

(d) Without Considering Cavitation Effects

* Distorted by the Bottom Reflection Wave

—— No Data or Not Calculated

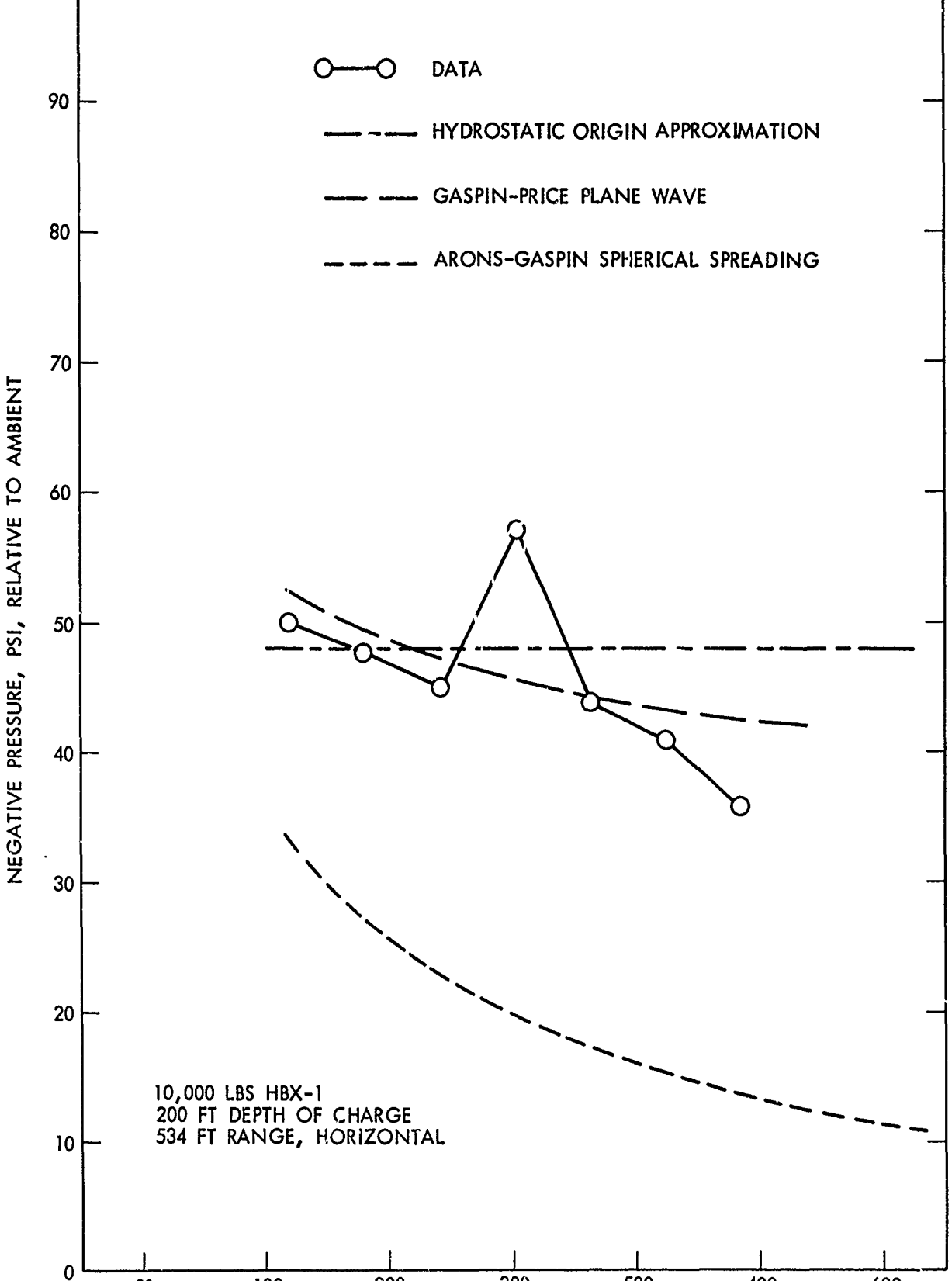

FIG. 7 MEASURED VS CALCULATED UNDERPRESSURES

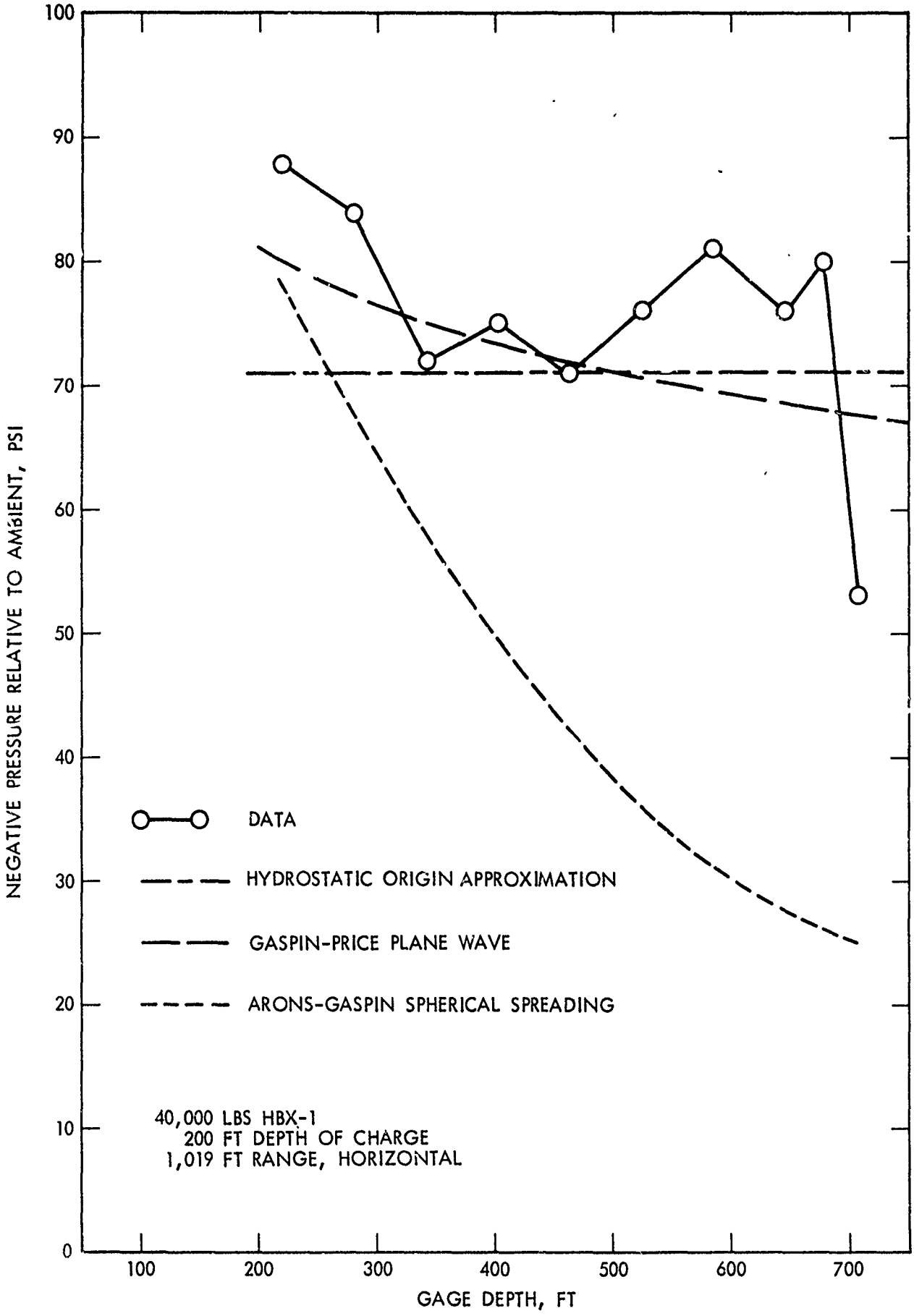

FIG. 8 MEASURED VS CALCULATED UNDERPRESSURES

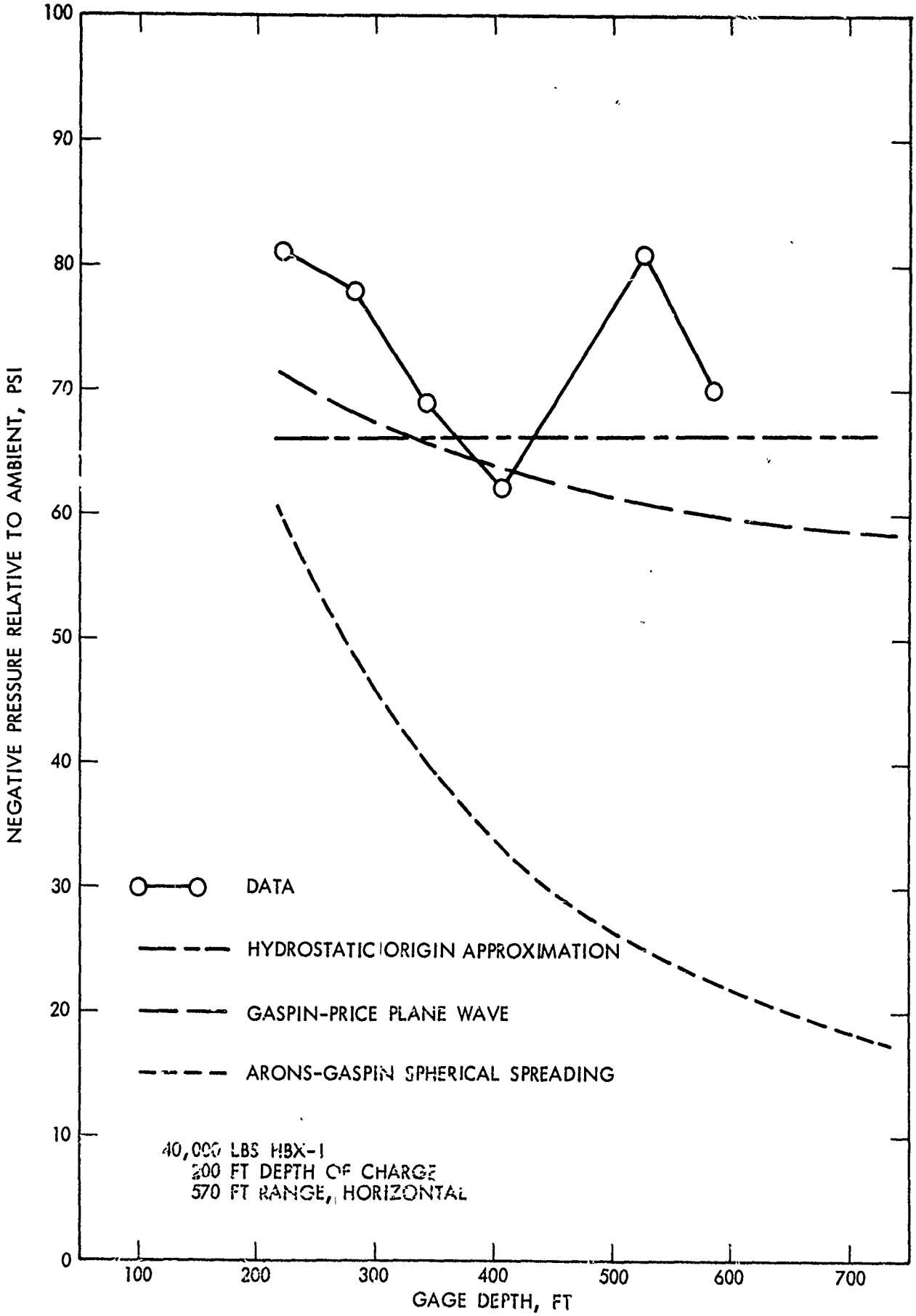

FIG. 9 MEASURED VS CALCULATED UNDERPRESSURES

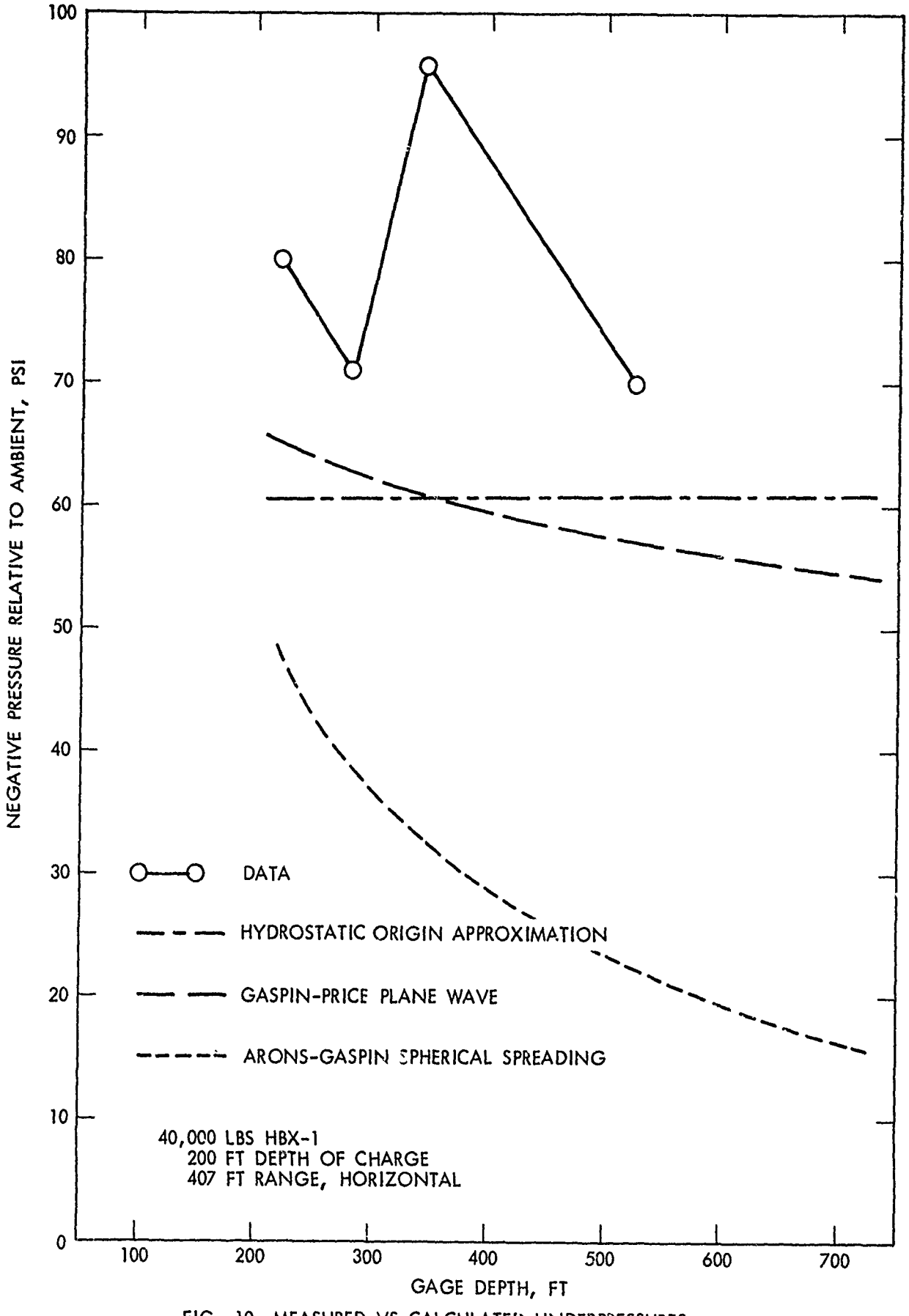

FIG. 10 MEASURED VS CALCULATED UNDERPRESSURES

6. REFERENCES

1. Arons, A. B., Yennie, D. R., and Cotter, T. P., "Long Range Shock Propagation in Underwater Explosion Phenomena II," in Underwater Explosions Compendium, Vol 1, 26 Oct 1949

2. Kennard, E. H., "Explosive Load on Underwater Structures as Modified by Bulk Cavitation," Taylor Model Basin Report No 511, May 1943

3. Kennard, E. H., "Cavitation in an Elastic Liquid," Phys Rev 63, 172 (1943)

4. Cushing, V., "Study of Bulk Cavitation and Consequent Water Hammer," Engineering Physics Company, Final Report on Contract NONR-3389(00), EPCO Project No 106, 31 Oct 1961.

   Cushing, V., et al., "Three Dimensional Analysis of Bulk Cavitation," Engineering Physics Company, Interim Report on Contract NONR-3709(00), EPCO Project No 106, 24 Sep 1962.

   Cushing, V., "On the Theory of Bulk Cavitation: Final Report," Engineering Physics Company, Contract NONR-3709(00), EPCO Project No 106, Dec 1969

5. Waldo, G. V., Jr., "A Bulk Cavitation Theory with a Simple Exact Solution," NSRDC Report 3010, Apr 1969

6. Walker, R. R., and Gordon, J. D., "A Study of the Bulk Cavitation Caused by Underwater Explosions," David Taylor Model Basin Report 1896, Sep 1966

7. Wentzell, R. A., et al, "Cavitation Due to Shock Pulses Reflected from the Sea Surface," Journal of the Acoustical Society of America, Vol 46, No 3, (Part 2), 789-794, Sep 1969

8. Snay, H. G., and Krieberl, A. R., "Surface Reflection of Underwater Shock Waves," NOLTR 70-31, 13 Mar 1970

APPENDIX A

COMPUTER PROGRAMS FOR CALCULATING BOUNDARY OF CAVITATED REGION

```
00100 REM READ K, ALPHA FØR PRESSURE
00110 READ K,A2
00120 REM READ K, ALPHA FØR THETA
00130 READ A3,A4
00140 REM ARØNS METHØD FØR CAVITATIØN
00150 REM W=CHG WT, LBS.
00160 REM D=CHG DEPTH, FT.
00170 REM R8=HØRIZØNTAL RANGE INCREMENT
00180 REM R9=MAX HØRIZØNTAL RANGE
00190 READ W,D,R8,R9
00200 LET P1=14.7
00210 LET H=.45
00220 LET C=5000
00230 PRINT"W="W,"DEPTH="D
00240 PRINT
00250 REM PRINTØUT IS HØR. RANGE AND DEPTH ØF CAV START AND STØP
00260 REM ALØNG A RAY FRØM IMAGE, AND MIN. ØF IMAGE WEIGHT
00270 PRINT"R START","Z START","R STØP","Z STØP","IMAGE WT"
00280 PRINT
00290 W2=W*(A2/3)
00300 H1=-R8
00310 I=0
00320 H1=H1+R8
00330 A=ATN(H1/D)
00340 IF H1>R9 THEN 01070
00350 LET R1=D/CØS(A)
00360 REM FIND W(IMAGE)=W
00370 LET I=I+1
00380 GØSUB 00680
00390 REM X=W(IMAGE)
00400 LET F=X-W2
00410 IF ABS(F)<1E-6 THEN 00480
00420 IF I>50 THEN 00460
00430 GØSUB 00780
00440 LET R1=R1-(F/X1)
00450 GØ TØ 00370
00460 PRINT"NØ CØNVERGENCE ØN CAV START"
00470 GØ TØ 01070
00480 LET Q1=R1*CØS(A)-D
00490 LET Q2=R1*SIN(A)
00500 REM FIND MIN ØF W(IMAGE)
00510 LET I=0
00520 LET I=I+1
00530 GØSUB 00780
00540 IF ABS(X1)<1E-6 THEN 00610
00550 IF I>50 THEN 00590
00560 GØSUB 00860
```

APPENDIX A (continued)

```
00570 LET R1=R1-(X1/X2)
00580 GØ TØ 00520
00590 PRINT"NØ CØNV ØN CAV STØP"
00600 GØ TØ 01070
00610 LET Q3=R1*CØS(A)-D
00620 LET Q4=R1*SIN(A)
00630 Q5=X↑(3/A2)
00640 PRINT Q2,Q1,Q4,Q3,Q5
00650 PRINT
00660 GØ TØ 00310
00670 REM CALCULATE W(IMAGE)
00680 LET R2=FNA(R1)
00690 LET B=FNB(R2)
00700 LET T=(R1-R2)/C
00710 LET G1=-T/B
00720 LET G2=EXP(G1)
00730 G3=G2*K*W2/(R2↑A2)
00740 LET G4=H*(R1*CØS(A)-D)
00750 X=(R1↑A2)*(P1+G4+G3)/K
00760 RETURN
00770 REM CALCULATE DERIV ØF W(IMAGE)...X1
00780 GØSUB 00680
00790 LET D1=FNC(R1)
00800 LET D2=FND(R1)
00810 L1=((R2/B)*D1)+A2*D2
00820 LET L2=L1*G3/R2
00830 X1=((R1↑A2)/K)*(H*CØS(A)-L2)+(A2*X/R1)
00840 RETURN
00850 REM CALCULATE2ND. DERIV ØF W(IMAGE)...X2
00860 D4=FNF(R1)
00870 LET D3=-D4/C
00880 M1=-(R1↑A2)*W2*G2/(R2↑(1+A2))
00890 M2=(R2*D3/B)+((D1*D2)/B)+A2*D4
00900 M3 =(R2*D1/B)+A2*D2
00910 M4=((R2*D1/B)+((A2+1)*D2))/R2
00920 M5=A2*R1↑(A2-1)*(H*CØS(A)-(G3/R2)*M3)/K
00930 LET M6=(R1*X1-X)/(R1↑2)
00940 M6 =M6*A2
00950 LET X2=M1*(M2-(M3*M4))+M5+M6
00960 RETURN
00970 REM FNA=R2
00980 DEF FNA(R1)=SQR(R1↑2+4*D↑2-4*D*R1*CØS(A))
00990 REM FNB=THETA
01000 DEF FNB(R)=A3*1E-3*W2*(W2/R)↑A4
01010 REM FNS C,D,E ARE INTERMEDIATE CALCS
01020 DEF FNC(R1)=(1-((R1-2*D*CØS(A))/R2))/C
01030 DEF FND(R1)=(R1-2*D*CØS(A))/R2
01040 DEF FNF(R1)=(K2-(K1-2*D*CØS(A))*D2)/R2↑2
01050 DATA 20800,1.13,.06,-.18
01060 DATA 40000,200,50,1100
01070 END
```

APPENDIX B

COMPUTER PROGRAM FOR CALCULATING UNDER PRESSURE BELOW CAVITATED REGION

```
00100 REM GASPIN-PRICE PLANE WAVE PROPAGATION
00110 REM       ALONG RAYS FROM IMAGE SOURCE.
00120 REM READ K, ALPHA FOR PRESSURE
00130 REM USE CONSTANTS TO OBTAIN PRESSURE IN PSI.
00140 READ K,A2
00150 REM READ K, ALPHA FOR THETA
00160 REM USE CONSTANTS TO OBTAIN TIME CONSTANT IN MILLISECONDS.
00170 READ A3,A4
00180 REM PROGRAM  CALCULATES UNDERPRESSURE FOR GAGE LOCATION
00190 REM      BELOW CAVITATED ZONE
00200 REM ARONS METHOD FOR CAVITATION
00210 REM  W=CHG WT,LBS.
00220 REM  D=CHG DEPTH,FT..
00230 REM H2=DESIRED GAGE HORIZ RANGE
00240 REM  D9=DESIRED GAGE DEPTH,FT.
00250 READ W,D
00260 PRINT"W="W,"DEPTH="D
00270 READ H2,D9
00280 LET P1=14.7
00290 LET H=.45
00300 LET C=5000
00310 PRINT
00320 W2=W^(A2/3)
00330 A=ATN(H2/(D+D9))
00340 LET R1=D/COS(A)
00350 I=0
00360 LET I=I+1
00370 GOSUB 00350
00380 LET F=X-W2
00390 IF ABS(F)<1E-6 THEN 00480
00400 IF I>50 THEN 00440
00410 GOSUB 00940
00420 LET R1=R1-(F/X1)
00430 GO TO 00360
00440 PRINT"NO CONVERGENCE ON CAV START"
00450 GO TO 09000
00460 PRINT "GAGE ABOVE CAVITATED REGION";G1
00470 GO TO 00500
00480 LET G1=R1*COS(A)-D
00490 IF D9<G1 THEN 00460
00500 LET G2=P1*SIN(A)
00510 LET I=0
00520 LET I=I+1
00530 GOSUB 00940
00540 IF ABS(X1)<1E-6 THEN 00630
00550 IF I>50 THEN 00590
00560 GOSUB 01010
00570 LET R1=R1-(X1/X2)
00580 GO TO 00520
```

APPENDIX B (continued)

```
00590 PRINT"NO CONV IN CAV STOP"
00600 GO TO 09000
00610 PRINT "GAGE IN OR ABOVE CAVITATED REGION";G3
00620 GO TO 00650
00630 LET G3=R1*COS(A)-D
00640 IF D9<G3 THEN 00610
00650 LET G4=R1*SIN(A)
00660 G5=X↑(3/A2)
00670 PRINT "IMAGE CHARGE WEIGHT"G5
00680 REM CALCULATE UNDERPRESSURE
00690 R3=R1
00700 Y1=K*X/(R1↑A2)
00710 M7=D-G3
00720 R4=G4
00730 T=(S1-P4)/C
00740 M8=-T/FNR(R4)
00750 M9=EXP(M8)
00760 P=M9*(K*W2/(R4↑A2)
00770 P9=P-Y1
00780 REM CALCULATE UNDERPRESSURE WITHOUT CAVITATION
00790 Y2=K*W2/(R3↑A2)
00800 P8=P-Y2
00810 PRINT"D GAGE="D9,"H GAGE="H2,"P NEG="P9,"PNEG NOCAV="P8
00820 PRINT"       P(T)="P;"T/THETA="M8
00830 PRINT
00840 GO TO 00270
00850 LET P2=FNA(R1)
00860 LET R=FNR(P2)
00870 LET T=(R1-R2)/C
00880 LET G1=-T/R
00890 LET G2=EXP(G1)
00900 G3=G2*(K*W2/(R2↑A2)
00910 LET G4=H*(R1*COS(A)-D)
00920 X=(R1↑A2)*(P1+G4+G3)/K
00930 RETURN
00940 GOSUB 00850
00950 LET D1=FNC(R1)
00960 LET D2=FND(R1)
00970 L1=((R2/R)*D1)+A2*D2
00980 LET L2=L1*G3/R2
00990 X1=((R1↑A2)/K)*(H*COS(A)-L2)+(A2*X/R1)
01000 RETURN
01010 D4=FNE(R1)
01020 LET D3=-D4/C
01030 M1=-(R1↑A2)*W2*G2/(P2↑(1+A2))
01040 M2=(P2*D3/R)+((D1*D2)/R)+A2*D4
01050 M3 =(R2*D1/S)+A2*D2
01060 M4=((R2*D1/R)+((A2+1)*D2))/R2
01070 M5=A2*P1↑(A2-1)*(H*COS(A)-(G3/R2)*M3)/K
```

APPENDIX B (continued)

```
01030 LET M6=(R1*X1-X)/(R1↑2)
01090 M6 =M6*A2
01100 LET X2=M1*(M2-(M3*M4))+M5+M6
01110 RETURN
01120 DEF FNA(R1)=SQR(R1↑2+4*D↑2-4*D*R1*COS(A))
01130 DEF FNB(R)=A3*1E-3*W2*(W2/R)↑A4
01140 DEF FNC(R1)=(1-((R1-2*D*COS(A))/R2))/C
01150 DEF FND(R1)=(R1-2*D*COS(A))/R2
01160 DEF FNE(R1)=(R2-(R1-2*D*COS(A))*D2)/R2↑2
01170 REM READ CONSTANTS: K,A2,A3,A4
01180 DATA 20050,1.09,.07,-.14
01190 REM READ CHARGE WEIGHT, CHARGE DEPTH.
01200 DATA 40000,200
01210 REM READ GAGE RANGES, GAGE DEPTHS (IN SETS):
01220 DATA 407,220
09000 END
```


EXAMPLE OF OUTPUT:

```
SJW232     14.54.19.  04/20/72


W= 40000        DEPTH= 200

IMAGE CHARGE WEIGHT 11.7265
D GAGE= 220    H GAGE= 407     P NEG=-64.9932 PNEG MICAV=-1363.31
       F(T)= 6.28313 T/THETA=-5.77874

END OF DATA   AT  270
14.54.23.BASIC EXECUTION TIME
CPU A=T
**READY.
```